Check for updates

Atmospheric Science Letters

RMetS Royal Meteorological Society

RESEARCH ARTICLE OPEN ACCESS

Exploring Clear-Sky Longwave Radiative Closure in the Arctic: A Downwelling Case Study

Sophie Mosselmans[1,2] | Helen Elizabeth Brindley[1,2] | Caroline Cox[3] | Edward Gryspeerdt[1] | Jonathan Murray[1,2] | Sanjeevani Panditharatne[1,2] | Laura Warwick[4] | Dirk Schuettemeyer[4] | Hilke Oetjen[4] | Tim Carlsen[5] | Andreas Foth[6] | Robert David[5]

[1]Department of Physics, Imperial College London, London, UK | [2]NERC National Centre for Earth Observation, Imperial College London, London, UK | [3]RAL Space, Harwell Oxford, Chilton, UK | [4]ESA-ESTEC, Noordwijk, the Netherlands | [5]Department of Geosciences, University of Oslo, Oslo, Norway | [6]Leipzig Institute for Meteorology, Leipzig University, Leipzig, Germany

Correspondence: Sophie Mosselmans (sophie.mosselmans19@imperial.ac.uk)

Received: 3 July 2025 | **Revised:** 2 October 2025 | **Accepted:** 6 November 2025

Keywords: field campaigns | humidity | observations | remote sensing | surface-based observations

ABSTRACT

The far infrared region plays a critical role in the Earth's greenhouse effect. Measurements across this range are limited and previous studies have found it challenging to achieve radiative closure between different instruments across the mid-far infrared. This study compares high-resolution downwelling spectra measured from the surface in the Arctic to radiative transfer simulations run with atmospheric profiles from a radiosonde, microwave radiometer, and the 5th ECMWF atmospheric reanalysis. The radiosonde-driven simulation generates the closest agreement to the radiance observations. The HATPRO-driven simulation matches within its uncertainty across the entire range. However, it has a larger uncertainty envelope than the other sources. There is a bias in all three simulations associated with underestimated humidity. Our results reiterate the sensitivity of the far infrared to the humidity profile. This suggests that the wider deployment of spectrometers capable of measuring across this region, in parallel with efforts to improve knowledge of far infrared water vapour spectroscopy, could markedly improve our ability to routinely characterise polar environments.

1 | Introduction

The IPCC has reported with high confidence that the rate of Arctic surface warming will continue to exceed the global average (Forster et al. 2021). Accurately quantifying the downwelling longwave flux is crucial for predicting the rates of this warming and the stability of ice surfaces in polar regions (Silber et al. 2019).

Typical Arctic near-surface air temperatures fall within the range 248–278 K resulting in a significant fraction of downwelling flux occurring within the far infrared (FIR) spectral region (15–100 μm or 100–667 cm^{-1}). At ground level, the atmosphere in the FIR spectral region is very opaque because of the high concentration of water vapour. Ground-based observations of the spectral distribution of downwelling radiances extending into the FIR are scarce (Palchetti et al. 2021). Those observations that are available have been used for atmospheric boundary layer temperature and humidity profiling (Belotti et al. 2023) but it has been demonstrated that it can be challenging to achieve radiative closure between different sounding instruments, even under clear-sky conditions (Liu et al. 2024).

Given the importance of the FIR and the scarcity of spectrally resolved measurements, the aim of this paper is to assess the degree to which clear-sky radiative closure can be achieved between ground-based spectrally resolved radiance observations and radiative transfer simulations extending across the far to mid-infrared. These simulations are driven by atmospheric profiles derived from a variety of different sources in an Arctic

This is an open access article under the terms of the Creative Commons Attribution License, which permits use, distribution and reproduction in any medium, provided the original work is properly cited.

© 2026 The Author(s). *Atmospheric Science Letters* published by John Wiley & Sons Ltd on behalf of the Royal Meteorological Society.

environment. We seek to determine the degree to which uncertainties in both the observations and the available modelling tools compromise our ability to obtain agreement, with a particular focus on the FIR region, given its strong sensitivity to water vapour vertical structure (Brindley and Harries 1998).

Downward longwave radiative flux (DLR) is a key component of the surface energy budget. Pan-Arctic DLR from the European Centre for Medium-Range Weather Forecasts Reanalysis v5 (ERA5; Hersbach et al. 2020) shows a notable positive trend over the last 30–40 years with winter-time seasonality primarily driven by near-surface temperature (Liu et al. 2025). However, estimates of DLR from observations, reanalyses (including ERA5) and models have particularly large uncertainties in the Arctic (L'Ecuyer et al. 2021). With this in mind, we also provide a simple assessment of the level of agreement in terms of downwelling flux to provide a clearer link to the impact of uncertainties in the atmospheric profile on the surface energy budget.

We use radiance observations from the Far INfrarEd Spectrometer for Surface Emissivity (FINESSE; Murray et al. 2024) which was built in support of the upcoming far infrared Outgoing Radiation Understanding and Monitoring (FORUM) mission, the European Space Agency's (ESA) 9th Earth Explorer, currently scheduled for launch in late 2027 (ESA 2022; Palchetti et al. 2020). FINESSE aims to help provide groundtruth datasets needed when FORUM flies. Although its primary purpose is to perform surface emissivity retrievals (Warwick et al. 2024), the instrument can also be used in purely zenith view mode, sampling the overhead conditions with high temporal resolution.

In February–March 2023, ESA supported the deployment of FINESSE to the Arctic LiDAR Observatory for Middle Atmosphere Research (ALOMAR) in Andøya, Norway to participate in the Mixed-phase Clouds and Climate ICE Pockets in Arctic Clouds at sub-Kilometre Scales (MC2 ICEPACKS) campaign, coordinated by the University of Oslo (David et al. in prep). The MC2-ICEPACKS campaign investigated the distribution of Arctic cloud phase with the aim of helping to further constrain Earth System Models. The campaign consisted of ground-based instruments and airborne measurements with support from the National Institute for Aerospace Research of Romania (INCAS) and the Atmospheric Research Laboratory (ATMOSLAB) aircraft. Alongside FINESSE, a multichannel microwave radiometer (Humidity And Temperature Profiler—HATPRO, generation 4) (Rose et al. 2005) and local radiosonde releases provided atmospheric state information. These were supplemented by reanalysis products from the ERA5 (Hersbach et al. 2020). Whilst, the campaign was focused on Arctic clouds, clear-sky conditions were also sampled. We exploit the only instance of these clear-sky observations that coincided with a local radiosonde launch to perform our radiative closure experiment. Clear-sky conditions were determined via visual sky inspection supplemented by examination of the FINESSE radiance spectra and variability in the atmospheric window region (780–1250 cm^{-1}). ERA5 reanalysis cloud cover at the nearest pixel also indicated clear-sky for that time.

2 | Instruments and Methods

The MC2-ICEPACKS campaign took place between 6th February and 17th March 2023 (David et al. in prep). This study focuses on clear sky observations taken at 0800 UTC on 8th March 2023. The location of the instruments used in this study is shown in Figure 1. FINESSE was based at 372 m above sea level and the HATPRO was located 1.9 km north-west of FINESSE at 5 m above sea level. A RS41-SGP radiosonde was launched at 08:00 UTC from Andenes airport at 5 m above sea level and 5.8 km north-east of FINESSE.

FINESSE comprises a Bruker EM27 Fourier transform spectrometer and a custom pointing and calibration system. It measures across the infrared spectrum (400–1600 cm^{-1}) with a spectral resolution of 0.5 cm^{-1} (Murray et al. 2024). On the day in question, FINESSE was operating in zenith mode and acquired interferograms every 1.5 s. To improve the signal-to-noise ratio, the data were averaged over 40 interferograms, resulting in an effective integration time of 1 min.

The HATPRO measures atmospheric emission at 14 frequencies; this signal is converted into voltages, which are calibrated

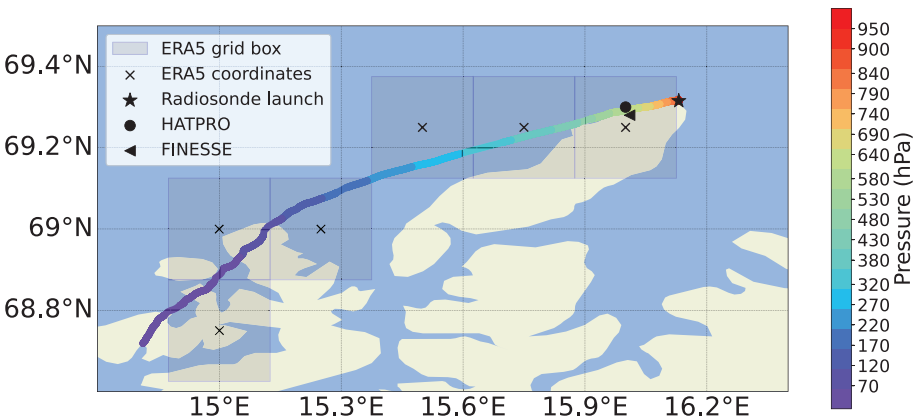


FIGURE 1 | Trajectory of 0800 UTC radiosonde launch from Andenes airport. The colour bar indicates the pressure level of the radiosonde at each point along its track. The shaded squares indicate ERA5 grid boxes through which the radiosonde passed. The black circle is the location of the microwave radiometer (HATPRO) and the black triangle is the location of FINESSE.

1530261x, 2026, 2, Downloaded from https://rmets.onlinelibrary.wiley.com/doi/10.1002/asl.70000 by Imperial College London, Wiley Online Library on [13/02/2026]. See the Terms and Conditions (https://onlinelibrary.wiley.com/terms-and-conditions) on Wiley Online Library for rules of use; OA articles are governed by the applicable Creative Commons License

into brightness temperatures (Löhnert and Maier 2012). A retrieval model, trained on a 20 year dataset of ERA5 atmospheric profiles, is used to transform the brightness temperatures into water vapour, temperature and humidity profiles. The general principles of the retrieval method are described in detail in Löhnert et al. (2007), and the particular approach used in this case is found within Foth et al. (2024).

Post launch, the radiosonde followed a south-westerly trajectory, passing closest to FINESSE at 08:11 UTC. By the time the radiosonde reached the second ERA5 grid box, it had ascended to 445 hPa (Figure 1). Above this level, the ERA5 profiles for humidity and temperature from the six grid boxes sampled by the radiosonde converge. For this reason, we use the single ERA5 profile centred at 69.25° N, 16.00° E in our subsequent simulations. The radiosonde burst at 13.30 hPa, and so ERA5 levels were used at higher altitudes.

Three baseline simulations were performed using atmospheric profiles from the radiosonde, HATPRO and ERA5 as sequential inputs to the Line-By-Line Radiative Transfer Model (LBLRTM; Clough 2014) version 12.13 with MT-CKD water vapour continuum model version 3.5. FINESSE has a Vaisala PTU300 sensor attached that measures pressure, temperature and relative humidity at the surface. These measurements were set as the surface boundary conditions for the radiosonde, ERA5 and HATPRO profile data. FINESSE also has a Vaisala GMP343 probe that measures CO_2 concentration, which was measured at 395 ppmv at 08:00 UTC. As CO_2 is a well-mixed greenhouse gas this concentration was assumed constant throughout the troposphere. The ozone profile for all of the simulations was taken from ERA5 reanalysis data. LBLRTM radiances were output at a resolution of 0.01 cm^{-1} before being apodised and convolved with the FINESSE instrument line shape. Both simulated and measured spectral radiances were multiplied by π to generate approximate estimates of spectral fluxes discussed later in the paper.

3 | Results

3.1 | Atmospheric Profiles

The humidity and temperature profiles from the three different sources are shown in Figure 2. There is notably better agreement between the temperature profiles than between the water profiles, with an average difference between ERA5 and the radiosonde of 0.06 K. Although the humidity profiles show good agreement between 550 and 150 hPa, they diverge significantly from each other between 830 and 600 hPa. In particular, the HATPRO retrieval shows a drier profile than either the radiosonde or ERA5 over this range. In contrast, between 900 and 830 hPa, the HATPRO retrieval is considerably more moist than the radiosonde and ERA5 profiles. Previous studies have noted that humidity profiling from HATPRO data is challenging due to their low information content (Blumberg et al. 2015; Walbröl et al. 2022). The radiosonde and ERA5 humidity profiles are generally well matched, with the exception of a humid layer around 800 hPa that is only present in the radiosonde profile.

While accurate profiling can be challenging, HATPROs typically provide more accurate assessments of Integrated Water Vapour (IWV) (Löhnert and Maier 2012). The IWV values from the different sources were as follows: 2.74 kg m^{-2} (HATPRO), 2.65 kg m^{-2} (ERA5) and 3.40 kg m^{-2} (Radiosonde). The compensating dry and moist biases result in the HATPRO IWV showing a reasonable agreement with the corresponding ERA5 value, however both are significantly drier than the radiosonde.

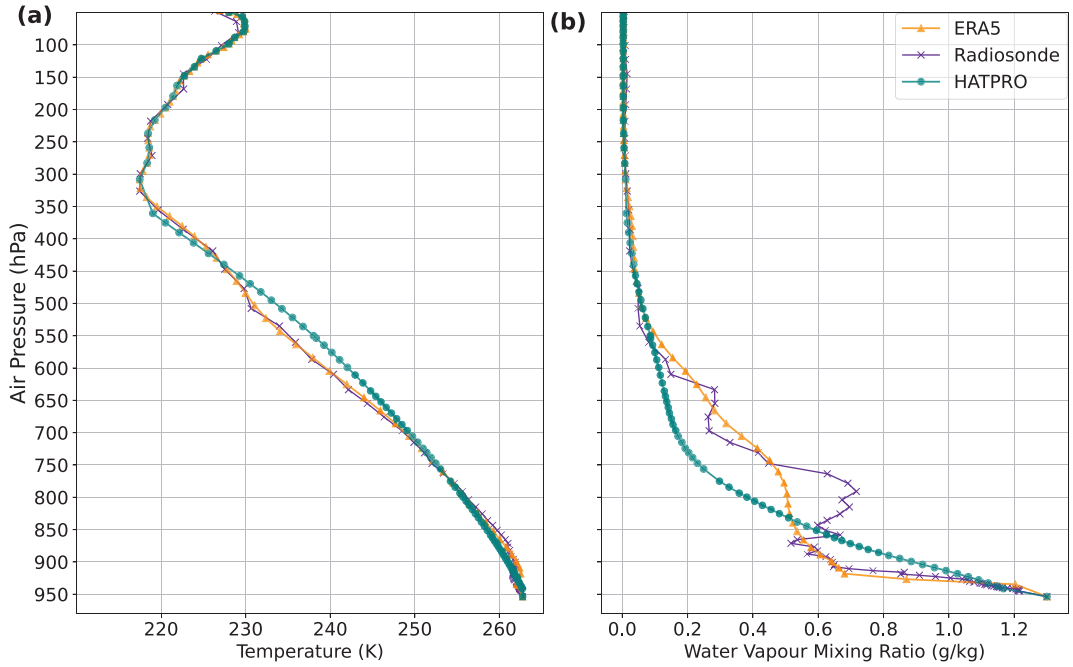


FIGURE 2 | (a) Temperature (K) and (b) water vapour mixing ratio (g/kg) as a function of pressure from the HATPRO (blue), ERA5 (orange) and radiosonde (purple). The surface values, at 954 hPa, were 1.30 g/kg and 262.7 K as measured by Vaisala sensors on FINESSE.

1530261x, 2026, 2, Downloaded from https://rmets.onlinelibrary.wiley.com/doi/10.1002/asl.70000 by Imperial College London, Wiley Online Library on [13/02/2026]. See the Terms and Conditions (https://onlinelibrary.wiley.com/terms-and-conditions) on Wiley Online Library for rules of use; OA articles are governed by the applicable Creative Commons License

3.2 | Radiance Uncertainties

As the quality of the ERA5 reanalysis data is variable, its ensemble members can be used to assess the contribution from uncertainties in the meteorological state (Hersbach et al. 2020). The ERA5 ensemble produces 10 different temperature and humidity profiles, which were used here to drive additional LBLRTM simulations. The standard deviation of the ensemble members' output radiance is used to approximate how uncertainties in the ERA5 profile propagate to radiance (Figure 3a).

To propagate the radiosonde uncertainties, minimum and maximum radiance profiles were constructed by applying the specified datasheet uncertainties (Vaisala 2020) to the original profile. For relative humidity this was 4%, for pressure 0.4 hPa, and for temperature 0.4 K. The uncertainty estimate was determined by calculating half the difference between the minimum and maximum radiance outputs from LBLRTM (Figure 3b). A similar approach was taken to derive the radiance uncertainties associated with the HATPRO retrieval. The HATPRO humidity and temperature profiles have a relatively low information content

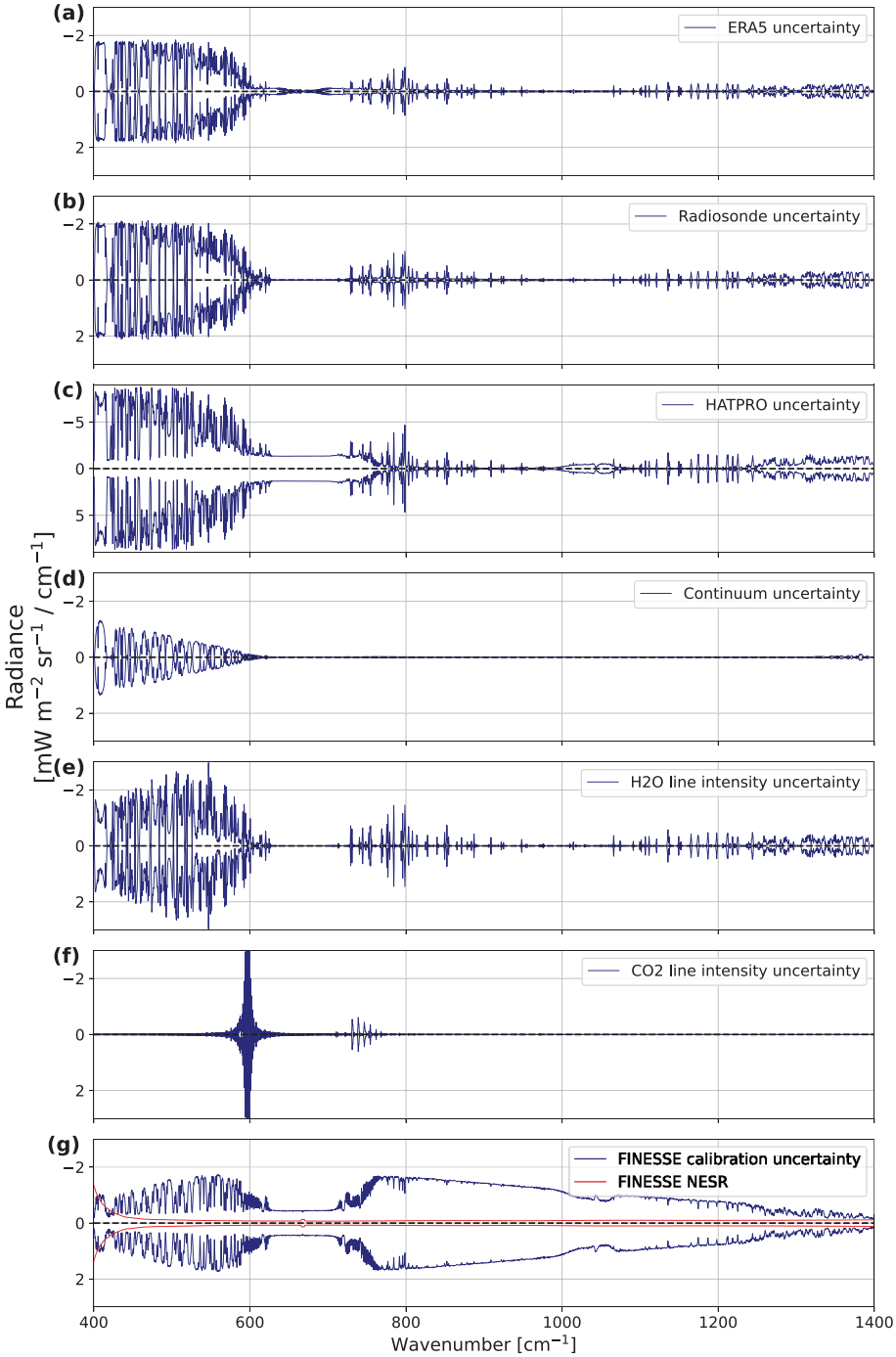


FIGURE 3 | Spectral uncertainties from LBLRTM simulations from the (a) ERA5 ensemble profiles standard deviation (b) radiosonde profile uncertainties, (c) HATPRO profile uncertainties, (d) foreign water vapour continuum uncertainties, (e) H_2O line intensity uncertainties, (f) CO_2 line intensity uncertainty and (g) FINESSE calibration uncertainties and Noise Equivalent Spectral Radiance (NESR) for the average spectrum. Note that radiances in (c) are on a different y-axis scale.

1530261x, 2026, 2, Downloaded from https://rmets.onlinelibrary.wiley.com/doi/10.1002/asl.70000 by Imperial College London, Wiley Online Library on [13/02/2026]. See the Terms and Conditions (https://onlinelibrary.wiley.com/terms-and-conditions) on Wiley Online Library for rules of use; OA articles are governed by the applicable Creative Commons License

with around 2 degrees of freedom, this causes uncertainties in the profiles (Walbröl et al. 2022). The retrieval's training data coefficients are applied to a set of test data to give uncertainty estimates. From these uncertainties, a constant absolute humidity bias of $-0.2\,\mathrm{kg\,m^{-3}}$ and temperature uncertainty of 1 K, were used to generate minimum and maximum radiances using LBLRTM (Figure 3c).

Errors in forward modelling, due, for example, to uncertainties in the water vapour continuum, have also been considered. Realistic uncertainties to the strength of the foreign water vapour continuum coefficients following Mlawer et al. (2019) were applied. The impact on the simulated radiances is shown in Figure 3d. Furthermore, the uncertainty in the spectral line intensity for water and carbon dioxide was taken into account. This was done by perturbing the values in the simulation according to their uncertainty estimates from HITRAN (Gordon et al. 2022) and calculating the difference to the original simulations. This is shown in Figure 3e,f. This was repeated for line position, but the calculated radiance uncertainty was negligible.

FINESSE uncertainties were derived from the calibration uncertainty and the Noise Equivalent Spectral Radiance (NESR). The calibration uncertainty was inferred from the accuracy of the platinum resistance thermometers, which monitor the temperatures of the hot and ambient blackbody calibration targets (Murray et al. 2024). The NESR is reduced by a factor of the square root of 40 as the data are averaged over 40 spectra. We then added this reduced NESR to the calibration uncertainty in quadrature to obtain a total measurement uncertainty estimate for FINESSE.

Figure 3 shows the magnitude of the radiance uncertainties associated with each source. For all three simulated cases (a-c), the uncertainties show similar spectral behaviour, being largest in the 400–600 $\mathrm{cm^{-1}}$ region, commonly referred to as the 'dirty window' (Mariani et al. 2012). As expected, the larger uncertainties in temperature and humidity in the HATPRO retrievals translate to a larger radiance uncertainty. The radiance uncertainties associated with a perturbation to the foreign water vapour continuum are minimal outside of the 400–600 $\mathrm{cm^{-1}}$ region and even here have about half the magnitude of those associated with the radiosonde and ERA5 temperature and humidity uncertainties. Uncertainties associated with H_2O line intensities are of a similar magnitude between 400 and 410 $\mathrm{cm^{-1}}$ but are larger throughout the majority of the dirty window, reaching a peak of close to $3\,\mathrm{mW\,m^{-2}\,sr^{-1}\,(cm^{-1})^{-1}}$ at 547 $\mathrm{cm^{-1}}$. Smaller uncertainties associated with individual lines and line clusters are also seen across the atmospheric window and within the vibration-rotation band. The CO_2 line intensity uncertainties are very prominent around 597 $\mathrm{cm^{-1}}$, extending to $7\,\mathrm{mW\,m^{-2}\,sr^{-1}\,(cm^{-1})^{-1}}$ (exceeding scale of figure). There are also some small spikes of uncertainty in the 700–800 $\mathrm{cm^{-1}}$ range. Propagated FINESSE uncertainties (g) have a somewhat different spectral shape to the other sources, with significant impacts seen in the atmospheric window—a consequence of the calibration uncertainty.

3.3 | Radiance Residuals

Radiance residuals between each of the three LBLRTM simulations (using ERA5, Radiosonde and HATPRO vertical profiles) and the FINESSE observations are shown in Figure 4. The associated uncertainties are derived by combining in quadrature the uncertainties derived for each profile (Figure 3a,b or c) with the spectroscopic uncertainties shown in Figure 3d–f and the FINESSE measurement uncertainty.

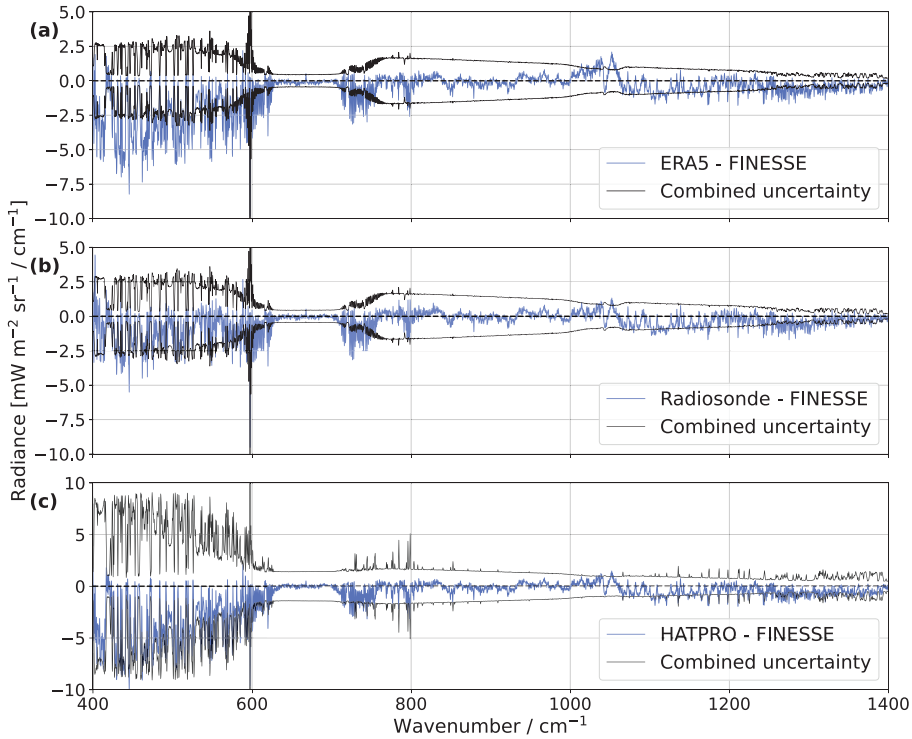


FIGURE 4 | Radiance residuals between FINESSE and LBLRTM simulations with atmospheric profiles sourced from ERA5 (a), a radiosonde (b) and a local HATPRO (c). The combined uncertainty comprises the respective spectral uncertainties (seen in Figure 3) added in quadrature.

1530261x, 2026, 2, Downloaded from https://rmets.onlinelibrary.wiley.com/doi/10.1002/asl.70000 by Imperial College London, Wiley Online Library on [13/02/2026]. See the Terms and Conditions (https://onlinelibrary.wiley.com/terms-and-conditions) on Wiley Online Library for rules of use; OA articles are governed by the applicable Creative Commons License

Simulation-observation radiance residuals using the HATPRO temperature and humidity profiles fall just within the boundary of the associated uncertainty limit across the entire 400–1400 cm^{-1} range (Figure 4c). However, this is predominantly a consequence of the significantly larger uncertainties associated with the retrieved profiles. Indeed, there is a pronounced mean bias of −3.68 $mW\,m^{-2}\,sr^{-1}\,(cm^{-1})^{-1}$ within the dirty window region. A smaller, but still apparent mean bias of −2.64 $mW\,m^{-2}\,sr^{-1}\,(cm^{-1})^{-1}$ is seen for the ERA5 simulation. However, in this case, the reduced uncertainty in the temperature and humidity profiles means that 'closure' is not achieved across the entire spectrum. Residuals exceed uncertainties in parts of the atmospheric window (800–1200 cm^{-1}), the dirty window, the water vapour vibration-rotation band at wavenumbers greater than 1250 cm^{-1} and the wings of the 667 cm^{-1} CO_2 band. For the radiosonde simulation, the magnitude of the mean bias is reduced even further, to −1.09 $mW\,m^{-2}\,sr^{-1}\,(cm^{-1})^{-1}$. A greater proportion of the residuals fall within the uncertainty bounds, compared to the ERA5 residuals.

These results suggest that the absence of the humid layer at 800 hPa in the ERA5 and HATPRO humidity profiles leads to a reduction in absorption and re-emission by water vapour, resulting in a lower simulated radiance compared to the simulation using the radiosonde profiles. Furthermore, while using the radiosonde profiles results in improved agreement with FINESSE radiances, the consistent remaining low bias in the dirty window and at wavenumbers greater than 1250 cm^{-1} suggests an even higher atmospheric moisture content was present above the spectrometer than that captured by the radiosonde.

As noted above, the radiance residuals for ERA5 and the radiosonde are larger than the uncertainty in the ν_2 CO_2 band wings between around 580–620 and 710–750 cm^{-1}. The bias in both cases is again negative. This implies that the lower troposphere is too cold in both sources or that the uncertainties in the lower tropospheric temperature profile are underestimated (Mariani et al. 2012). A sharp residual is present at 597 cm^{-1}, which spectroscopic perturbations indicate is due to issues with the representation of line coupling in the CO_2 Q-branch within LBLRTM (Delamere et al. 2010; Filippov et al. 2002). The perturbations to CO_2 line strengths also produce a spike centred on this wavenumber (3f).

3.4 | Impact on Downwelling Longwave Surface Flux

The spectral radiances were multiplied by π to convert to downwelling spectral flux. Ideally, one would account for variations in anisotropic factor with atmospheric opacity, but this conversion gives a first-order approximation, which is sufficient to draw the main conclusions here. Figure 5 indicates the energetic impact of the differences between the simulations and observations by comparing the resulting downwelling fluxes integrated over the spectral range 400–1400 cm^{-1}. This region comprises approximately 56% of the total downwelling flux between 0 and 2500 cm^{-1}. Consistent with the radiance residuals, all of the simulations underestimate the flux compared to FINESSE, with differences of 3.10 ± 4.91 $W\,m^{-2}$ (HATPRO), 2.49 ± 2.85 $W\ m^{-2}$ (ERA5) and 1.09 ± 2.72 $W\ m^{-2}$ (Radiosonde).

To further investigate these discrepancies we decomposed the fluxes into different spectral regions covering the FIR (400–667 cm^{-1}); part of the ν_2 CO_2 band (667–800 cm^{-1}); atmospheric window (800–980 and 1100–1250 cm^{-1}); ozone band (980–1100 cm^{-1}) and water vapour ν_2 band wing (1250–1400 cm^{-1}) (Figure 5). As might be anticipated from Figure 4, the majority of the bias (~72%) is seen within the FIR 400–667 cm^{-1} range, with much smaller deviations outside of this region. The vertical tick marks on each bar in Figure 5 are combined uncertainties. These were estimated by multiplying the combined uncertainties shown in Figure 4 by π and integrating over the spectral ranges.

4 | Conclusions

In this paper, we use ground-based radiance observations made by the FINESSE spectrometer during the MC2-ICEPACKS campaign out of Andøya, Norway to assess the degree to which clear-sky radiative closure can be obtained using a

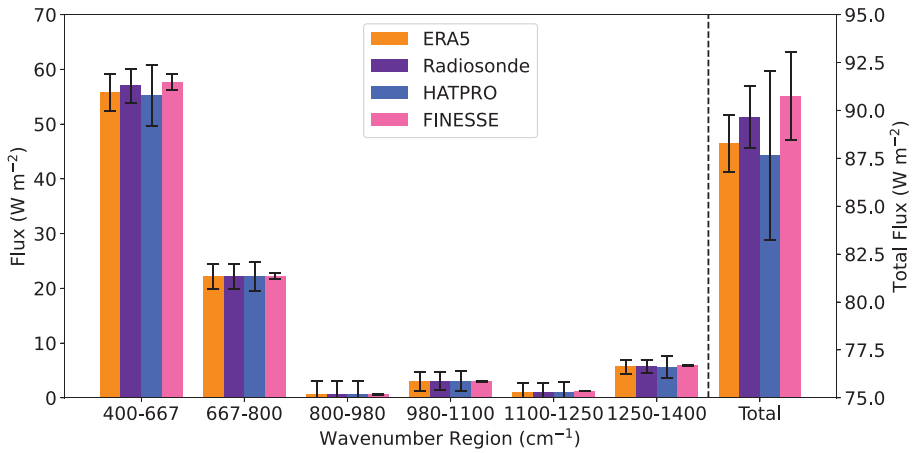


FIGURE 5 | Surface downwelling fluxes ($W\,m^{-2}$) integrated over different spectral regions for ERA5 (orange), Radiosonde (purple), HATPRO (blue) and FINESSE (pink). For comparison, the total flux over the range 400–1400 cm^{-1} is also shown. The vertical tick marks on each bar are combined uncertainties.

1530261x, 2026, 2, Downloaded from https://rmets.onlinelibrary.wiley.com/doi/10.1002/asl.70000 by Imperial College London, Wiley Online Library on [13/02/2026]. See the Terms and Conditions (https://onlinelibrary.wiley.com/terms-and-conditions) on Wiley Online Library for rules of use; OA articles are governed by the applicable Creative Commons License

variety of observational and reanalysis tools. Specifically, we use profiles measured by an RS41-SGP radiosonde, derived from a HATPRO and extracted from ERA5 reanalyses, in conjunction with the LBLRTM radiative transfer model. There are several sources of uncertainty, arising from the measurement of profiles and the radiative transfer model. The spectroscopic uncertainty in H_2O line intensities has a relatively large contribution to the total uncertainty in this case, something which is often unaccounted for within closure studies (e.g., Liu et al. (2024)). Future work to investigate whether the quoted spectroscopic uncertainties in the relatively unexplored FIR are representative of the true state of knowledge would therefore be beneficial.

The HATPRO matches the observed radiances within the associated uncertainty budget across the entire 400–1400 cm^{-1} range. However, the HATPRO has a significantly larger uncertainty envelope than the other sources. In the HATPRO drive simulation, there is a particularly significant low bias manifested in the FIR part of the spectrum between 400 and 667 cm^{-1}. This bias is smaller but still present in the ERA5-driven simulation, which does not match the observations within its uncertainty budget. The profile measured by the radiosonde generates the closest agreement to the radiance observations despite its launch location being markedly further away from FINESSE than the HATPRO. The radiosonde also has a small bias in the 400–667 cm^{-1}. In common with other studies, the HATPRO retrievals are unable to capture the detailed atmospheric vertical profile (Blumberg et al. 2015; Walbröl et al. 2022). Furthermore, in line with previous studies (Löhnert and Maier 2012), the IWV amount from the HATPRO is more aligned to that obtained from the closest ERA5 reanalysis profile, but both significantly underestimate IWV compared to the radiosonde.

By translating radiance to an approximated flux, we find that the clear sky downwelling surface fluxes simulated from the HATPRO profiles are up to 3.10 $W m^{-2}$ smaller than those obtained from FINESSE when integrated over the 400–1400 cm^{-1} range. The equivalent underestimates from ERA5 and the radiosonde derived profiles are 2.49 and 1.09 $W m^{-2}$, respectively. Previous studies have noted a low bias in ERA5 clear-sky downwelling longwave surface fluxes over polar sites (Guo et al. 2024; Silber et al. 2019) which is consistent with our findings here. By decomposing spectrally we are able to show that the majority of the underestimate occurs within the FIR and, in this case, is linked to an inability to capture a relatively narrow near-surface moist layer.

Our results provide a further demonstration of how ground-based spectrally resolved radiances can be used to assess the performance of commonly used observational and reanalyses tools. They highlight the difficulties in obtaining radiative closure, under relatively well-constrained conditions. They also demonstrate the sensitivity of the FIR region of the spectrum to vertical detail in the overlying water vapour profile and suggest that the wider deployment of spectrometers capable of measuring across this region could markedly improve our ability to routinely characterise polar environments while simultaneously linking the evolution of the atmospheric state to its energetic impact.

Author Contributions

Sophie Mosselmans: writing – original draft, writing – review and editing, methodology, validation, visualization, investigation, formal analysis, data curation, software. **Helen Elizabeth Brindley:** investigation, funding acquisition, writing – review and editing, conceptualization, supervision, project administration. **Caroline Cox:** writing – review and editing, supervision. **Edward Gryspeerdt:** writing – review and editing, supervision. **Jonathan Murray:** methodology, conceptualization, formal analysis, supervision, project administration. **Sanjeevani Panditharatne:** supervision, writing – review and editing. **Laura Warwick:** supervision, writing – review and editing. **Dirk Schuettemeyer:** funding acquisition, project administration. **Hilke Oetjen:** funding acquisition, project administration. **Tim Carlsen:** methodology, resources. **Andreas Foth:** methodology, resources. **Robert David:** methodology, resources.

Acknowledgements

The authors would like to thank the MC2-ICEPACKS campaign support team. Thanks to Martin Flugge for facilitating the deployment of FINESSE, the Met sounding team (Terje Borge, Baard Meldal-Johnsen and Kjetil Stiansen) for launching radiosondes during the observing period.

Funding

European Space Agency funded the deployment of FINESSE to Andoya. R.O.D. and T.C. gratefully acknowledge the funding by the European Research Council (ERC) through Starting Grant 758005 (Mixed-phase clouds and climate-MC2), Consolidator Grant 101045273 (STEP-CHANGE) and through EU-HORIZON-WIDERA-2021 Grant 101079385 (BRACE-MY). R.O.D. would also like to acknowledge EEARO-NO-2019-0423/IceSafari, Contract 31/2020, under the NO Grants 2014–2021 of EEA Grants/Norway Grants. Sophie Mosselmans was funded by NERC via the SSCP DTP. E.G. was supported by a Royal Society University Research Fellowship and renewal (URF/R1/191602, URF/R/241017). H.E.B. and J.E.M. are supported by the Natural Environment Research Council under grant no. NE/Y006216/1.

Conflicts of Interest

The authors declare no conflicts of interest.

Data Availability Statement

The FINESSE Andøya campaign data is available online via the ESA EO Gateway, follow: https://doi.org/10.57780/esa-e8a8e82.

Radiosonde Data is available, under Observations and then Remote sensing, on the following link: https://thredds.met.no/thredds/catalog.html.

ERA5 reanalysis data was downloaded from the Copernicus Climate Data Store.

HATPRO retrievals are public on github: https://github.com/remsens-lim/pyMakeRetrieval. The HATPRO data used in this paper is available upon request. Permission to use HATPRO data from Tim, Andreas and Rob.

References

Belotti, C., F. Barbara, M. Barucci, et al. 2023. "The Far-Infrared Radiation Mobile Observation System (FIRMOS) for Spectral Characterization of the Atmospheric Emission." *Atmospheric Measurement Techniques* 16, no. 10: 2511–2529. https://doi.org/10.5194/amt-16-2511-2023.

Blumberg, W. G., D. D. Turner, U. Löhnert, and S. Castleberry. 2015. "Ground-Based Temperature and Humidity Profiling Using Spectral

1530261x, 2026, 2, Downloaded from https://rmets.onlinelibrary.wiley.com/doi/10.1002/asl.70000 by Imperial College London, Wiley Online Library on [13/02/2026]. See the Terms and Conditions (https://onlinelibrary.wiley.com/terms-and-conditions) on Wiley Online Library for rules of use; OA articles are governed by the applicable Creative Commons License

Infrared and Microwave Observations. Part II: Actual Retrieval Performance in Clear-Sky and Cloudy Conditions." *Journal of Applied Meteorology and Climatology* 54, no. 11: 2305–2319. https://doi.org/10.1175/JAMC-D-15-0005.1.

Brindley, H. E., and J. E. Harries. 1998. "The Impact of Far i.r. Absorption on Clear Sky Greenhouse Forcing: Sensitivity Studies at High Spectral Resolution." *Journal of Quantitative Spectroscopy & Radiative Transfer* 60, no. 2: 151–180. https://doi.org/10.1016/S0022-4073(97)00152-0.

Clough, S. A. 2014. "LBLRTM: Line-By-Line Radiative Transfer Model." Retrieved May 16, 2024. https://ui.adsabs.harvard.edu/abs/2014ascl.soft05001C.

Delamere, J. S., S. A. Clough, V. H. Payne, E. J. Mlawer, D. D. Turner, and R. R. Gamache. 2010. "A Far-Infrared Radiative Closure Study in the Arctic: Application to Water Vapor." *Journal of Geophysical Research: Atmospheres* 115, no. D17: 10–11. https://doi.org/10.1029/2009JD012968.

ESA. 2022. "Forum Mission Science Plan (Science Plan No. Issue 1.0)." Earth and Mission Science Division, July.

Filippov, N. N., V. P. Ogibalov, and M. V. Tonkov. 2002. "Line Mixing Effect on the Pure CO2 Absorption in the 15 Micron Region." *Journal of Quantitative Spectroscopy & Radiative Transfer* 72, no. 4: 315–325. https://doi.org/10.1016/S0022-4073(01)00124-8.

Forster, P., T. Storelvmo, K. Armour, et al. 2021. "The Earth's Energy Budget, Climate Feedbacks, and Climate Sensitivity." In *Climate Change 2021: The Physical Science Basis. Contribution of Working Group I to the Sixth Assessment Report of the Intergovernmental Panel on Climate Change (Tech. Rep.)*. Cambridge University Press. retrieved September 21, 2024. https://www.ipcc.ch/report/ar6/wg1/chapter/chapter-7/.

Foth, A., M. Lochmann, P. Saavedra Garfias, and H. Kalesse-Los. 2024. "Determination of Low-Level Temperature Profiles From Microwave Radiometer Observations During Rain." *Atmospheric Measurement Techniques* 17, no. 24: 7169–7181. https://doi.org/10.5194/amt-17-7169-2024.

Gordon, I. E., L. S. Rothman, R. J. Hargreaves, et al. 2022. "The HITRAN2020 Molecular Spectroscopic Database." *Journal of Quantitative Spectroscopy & Radiative Transfer* 277: 107949. https://doi.org/10.1016/j.jqsrt.2021.107949.

Guo, M., J. Cheng, and Q. Zeng. 2024. "A Data-Driven Model for Estimating Clear-Sky Surface Longwave Downward Radiation Over Polar Regions." *IEEE Transactions on Geoscience and Remote Sensing* 62: 1–13. https://doi.org/10.1109/TGRS.2024.3418205.

Hersbach, H., B. Bell, P. Berrisford, et al. 2020. "The ERA5 Global Reanalysis." *Quarterly Journal of the Royal Meteorological Society* 146, no. 730: 1999–2049. https://doi.org/10.1002/qj.3803.

L'Ecuyer, T. S., B. J. Drouin, J. Anheuser, et al. 2021. "The Polar Radiant Energy in the Far Infrared Experiment: A New Perspective on Polar Longwave Energy Exchanges." *Bulletin of the American Meteorological Society* 102: E1431–E1449. https://doi.org/10.1175/BAMS-D-20-0155.1.

Liu, L., N. Bliankinshtein, Y. Huang, et al. 2024. "Radiative Closure Tests of Collocated Hyperspectral Microwave and Infrared Radiometers." *Atmospheric Measurement Techniques* 17, no. 7: 2219–2233. https://doi.org/10.5194/amt-17-2219-2024.

Liu, Y., H. Li, Y. He, and Y. Liu. 2025. "Seasonal Shifts in Pan-Arctic Ocean Downward Radiation and Key Drivers." *iScience* 28, no. 9: 113399. https://doi.org/10.1016/j.isci.2025.113399.

Löhnert, U., and O. Maier. 2012. "Operational Profiling of Temperature Using Ground-Based Microwave Radiometry at Payerne: Prospects and Challenges." *Atmospheric Measurement Techniques* 5, no. 5: 1121–1134. https://doi.org/10.5194/amt-5-1121-2012.

Löhnert, U., E. van Meijgaard, H. K. Baltink, S. Groß, and R. Boers. 2007. "Accuracy Assessment of an Integrated Profiling Technique for Operationally Deriving Profiles of Temperature, Humidity, and Cloud Liquid Water." *Journal of Geophysical Research: Atmospheres* 112, no. D4: 1–17. https://doi.org/10.1029/2006JD007379.

Mariani, Z., K. Strong, M. Wolff, et al. 2012. "Infrared Measurements in the Arctic Using Two Atmospheric Emitted Radiance Interferometers." *Atmospheric Measurement Techniques* 5, no. 2: 329–344. https://doi.org/10.5194/amt-5-329-2012.

Mlawer, E. J., D. D. Turner, S. N. Paine, et al. 2019. "Analysis of Water Vapor Absorption in the Far-Infrared and Submillimeter Regions Using Surface Radiometric Measurements From Extremely Dry Locations." *Journal of Geophysical Research: Atmospheres* 124, no. 14: 8134–8160. https://doi.org/10.1029/2018JD029508.

Murray, J. E., L. Warwick, H. Brindley, et al. 2024. "The Far INfrarEd Spectrometer for Surface Emissivity (FINESSE). Part 1: Instrument Description and Level 1 Radiances." *Atmospheric Measurement Techniques* 17: 4757–4775. https://doi.org/10.5194/amt-2024-22.

Palchetti, L., M. Barucci, C. Belotti, et al. 2021. "Observations of the Downwelling Far-Infrared Atmospheric Emission at the Zugspitze Observatory." *Earth System Science Data* 13, no. 9: 4303–4312. https://doi.org/10.5194/essd-13-4303-2021.

Palchetti, L., H. Brindley, R. Bantges, et al. 2020. "FORUM: Unique Far-Infrared Satellite Observations to Better Understand How Earth Radiates Energy to Space." *Bulletin of the American Meteorological Society* 101, no. 12: E2030–E2046. https://doi.org/10.1175/BAMS-D-19-0322.1.

Rose, T., S. Crewell, U. Löhnert, and C. Simmer. 2005. "A Network Suitable Microwave Radiometer for Operational Monitoring of the Cloudy Atmosphere." *Atmospheric Research* 75, no. 3: 183–200. https://doi.org/10.1016/j.atmosres.2004.12.005.

Silber, I., J. Verlinde, S.-H. Wang, et al. 2019. "Cloud Influence on ERA5 and AMPS Surface Downwelling Longwave Radiation Biases in West Antarctica." *Journal of Climate* 32: 7935–7949. https://doi.org/10.1175/JCLI-D-19-0149.1.

Vaisala. 2020. "RS41 Upper Air Radiosonde – Vaisala." Retrieved November 18, 2024, from https://www.vaisala.com/en/products/weather-environmental-sensors/upper-air-radiosondes-rs41-rs41-e-models.

Walbröl, A., S. Crewell, R. Engelmann, et al. 2022. "Atmospheric Temperature, Water Vapour and Liquid Water Path From Two Microwave Radiometers During MOSAiC." *Scientific Data* 9, no. 1: 534. https://doi.org/10.1038/s41597-022-01504-1.

Warwick, L., J. E. Murray, and H. Brindley. 2024. "The Far-INfrarEd Spectrometer for Surface Emissivity (FINESSE) – Part 2: First Measurements of the Emissivity of Water in the Far-Infrared." *Atmospheric Measurement Techniques* 17, no. 16: 4777–4787. https://doi.org/10.5194/amt-17-4777-2024.

1530261x, 2026, 2, Downloaded from https://rmets.onlinelibrary.wiley.com/doi/10.1002/asl.70000 by Imperial College London, Wiley Online Library on [13/02/2026]. See the Terms and Conditions (https://onlinelibrary.wiley.com/terms-and-conditions) on Wiley Online Library for rules of use; OA articles are governed by the applicable Creative Commons License